

**Supporting information**

**One-step fabrication of electrospun flexible and hierarchically porous Pt/ $\gamma$ -Al<sub>2</sub>O<sub>3</sub>  
nanofiber membrane for HCHO and particulate removal**

Sitian Xin, Silong Zhu, Jianfei Zheng, Longhui Nie\*

*(Hubei Provincial Key Laboratory of Green Materials for Light Industry, Hubei University of Technology, Wuhan 430068, China; Collaborative Innovation Center of Green Light-weight Materials and Processing, Hubei University of Technology, Wuhan 430068, China.)*

\* Author to whom any correspondence should be addressed. E-mail:

nielonghui@mail.hbut.edu.cn (L. Nie)

## 1. Characterization

The phase composition of the samples was analyzed on an Empyrean X-ray powder diffractometer (PANalytical, Netherlands) (working parameters: the test voltage: 45 kV, the current: 40 mA, the wavelength  $\lambda$ : 0.15406 nm, and the scanning range  $2\theta$ :  $10^\circ$ - $80^\circ$ ). The microscopic morphologies of the samples were examined on a scanning electron microscope (SEM, SU8010, Hitachi) with 2.0 kV working voltage and a transmission electron microscope (TEM, EOL2100F) with 200 kV working voltage. The element composition and valence states of the samples were conducted on an X-ray photoelectron spectroscopy (XPS, VG ESCALAB250xi) with Al  $K\alpha$  as the X-ray source (1486.7 eV), and the binding energies of elements in the samples were calibrated with the reference to the surface contamination carbon (C1s, 284.8 eV). The  $N_2$  adsorption/desorption isotherms of the samples were acquired on an ASAP 2020 (Micromeritics, USA) adsorption and desorption device, and the BET specific surface areas ( $S_{BET}$ ) for the samples could be computed from the results of  $N_2$  adsorption and desorption. All samples were pretreated at 180 °C for 4 h before examining. The pore size distribution curves of the samples were acquired from the data of the adsorption branch using the BJH method. The single-point nitrogen adsorption results at  $P/P_0 = 0.98$  were used to calculate the pore volume and average pore diameter of the samples. The analysis of the surface species of the sample before and after HCHO oxidation was carried out on a Fourier transform infrared spectrometer (FTIR, Nicolet 6700, Thermo Fisher) with working parameters: the scanning wave number range = 4000-400  $cm^{-1}$ , the scanning speed = 0.2  $cm \cdot s^{-1}$ , and

the number of scans = 16 times).

The analysis of the intermediates during HCHO oxidation over PAO was conducted on a Thermo Fisher 6700 instrument through *In situ* diffuse reflectance infrared Fourier transformations spectroscopy (*in situ* DRIFTS) technique. The sample was pretreated at 120 °C for 2 h in *in situ* cell reactor under a gas flow of N<sub>2</sub>. And then, the gas mixture (30 mL·min<sup>-1</sup> of HCHO (80 ppm)/N<sub>2</sub>, O<sub>2</sub>, or HCHO (80 ppm)/O<sub>2</sub> controlled by a mass flow controller (MFC)) were introduced into the *in situ* DRIFTS cell under the ambient temperature in proper order. All the *situ* DRIFTS spectra were obtained after subtracting the background. Scanning range was from 4000 to 650 cm<sup>-1</sup> with a resolution of 4 cm<sup>-1</sup>.

## **2. Catalytic activity and stability for HCHO oxidation**

The evaluation of catalytic activities of the samples for HCHO oxidation at room temperature was described as the same as our previous work [1]. Typically, 0.1 g of sample was placed at the bottom of a glass petri dish with a lid. A certain amount of HCHO solution is injected into the reactor. After establishing the adsorption equilibrium, the initial concentration of HCHO (detected by a PN-2000-CH<sub>2</sub>O formaldehyde gas detector, Shenzhen Peng Lei Technology Co., Ltd.) was controlled to be about ~ 125 ppm, and then removed the glass lid to start reaction. The concentration of CO<sub>2</sub> product was determined by gas chromatography (GC, 9790 II, Fuli) with a methane converter. The reaction temperature and relative humidity were maintained to be about ~ 25 °C and ~50%, respectively. The evaluation of catalytic activity for the samples was carried out by the reducing HCHO concentration and the

increasing CO<sub>2</sub> concentration ( $\Delta\text{CO}_2$ ) in 60 min for each test.

### 3. Evaluation of filtration performance and fluid permeability

The filtration performance of the sample for water was evaluated by filtrating the simulated particulate matters of the SiO<sub>2</sub> or C spheres (the mean diameter of ca. 763 nm and 368 nm for SiO<sub>2</sub> or C spheres, respectively, determined by a laser particle analyzer (Zeta plus, Brookhaven)) in water. Typically, 20 mg of SiO<sub>2</sub> or C spheres were dispersed in deionized H<sub>2</sub>O (100 ml). The PAO2 sample (9.35 mg·cm<sup>-2</sup>) was taken to filtrate the above suspensions (30 mL). The turbidities of the solutions before (diluted 10 times before testing) and after filtration were determined using a WZS-B turbidity meter (Hangzhou Qiwei Instrument Co., Ltd.).

To investigate the fluid permeability, the pure water flux of the sample was detected on a cross-flow filtration equipment with three sample cells (SF-SA, Saifei Membrane Separation Limited Corporation of Hangzhou, China, effective membrane area of ca. 21.2 cm<sup>2</sup>) at room temperature. 2.0 L of fresh de-ionized water was used to flush the filtration equipment under 0.1 MPa transmembrane pressure for three times within 5 min. The pure water flux of the sample ( $J$ ) can be obtained by the following equation:

$$J = V / (A \cdot t)$$

Where  $J$  (L·(m<sup>2</sup>·h)<sup>-1</sup>) is the pure water flux;  $A$  (m<sup>2</sup>) is the area of nanofiber paper, and  $t$  (h) is the sampling time;  $V$  (L) is the volume of the permeated water.

### 4. Results

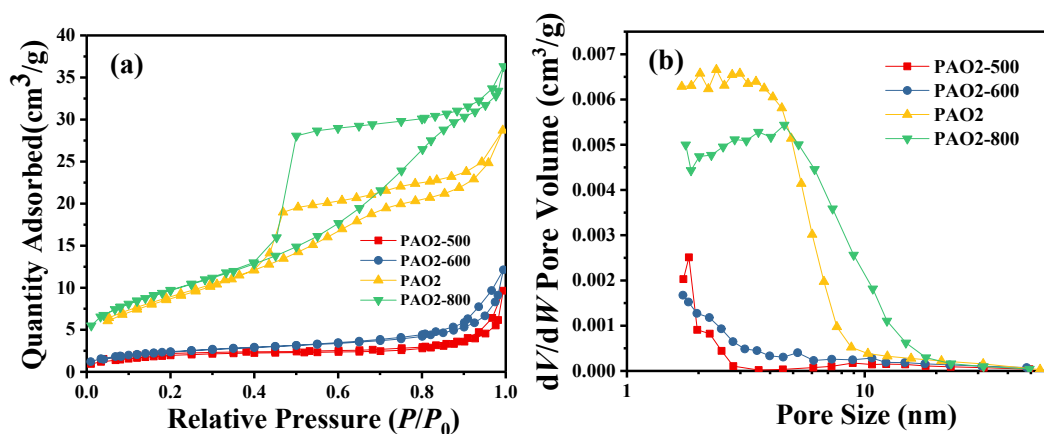


Figure S1 N<sub>2</sub> adsorption-desorption isotherms (a) and the corresponding pore size distribution curves (b) of the PAO2-500, PAO2-600, PAO2 and PAO2-800 samples.

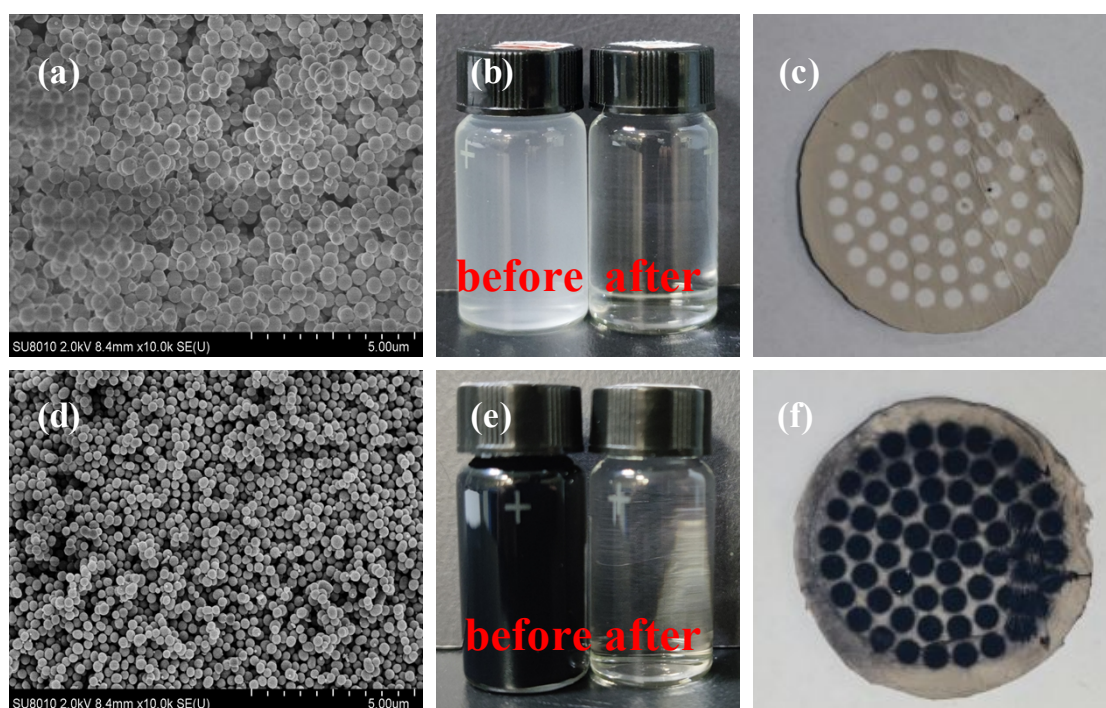


Figure S2 SEM images of simulated particles of SiO<sub>2</sub> and C spheres (a, d), optical images of suspension before and after filtration by PAO2 (b, e), and physical images after membrane filtration (c, f)

[1] S. Zhu, J. Zheng, S. Xin and L. Nie, Chem. Eng. J., 2021, 427, 130951.